

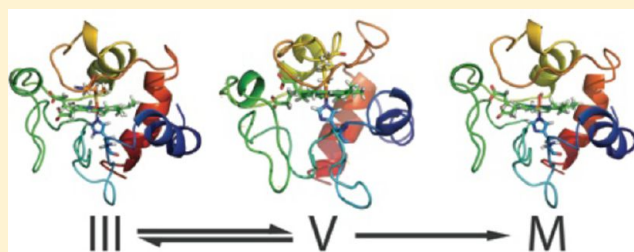
The (Not Completely Irreversible) Population of a Misfolded State of Cytochrome *c* under Folding Conditions

Jonathan B. Soffer, Emma Fradkin, Leah A. Pandiscia, and Reinhard Schweitzer-Stenner*

Departments of Chemistry and Biology, Drexel University, 3141 Chestnut Street, Philadelphia, Pennsylvania 19104, United States

S Supporting Information

ABSTRACT: This paper reports the discovery of a (meta)-stable partially unfolded state of horse heart ferricytochrome *c* that was obtained after exposing the protein to a solution with an alkaline pH of 11.5 for 1 week. Thereafter, the protein did not undergo any detectable change in its secondary and tertiary structure upon adjusting the solution to folding promoting conditions at neutral pH. Spectroscopic data suggest that the misfolded protein exhibits a hexacoordinated low-spin state with a hydroxyl ion as the likely ligand. Below pH 6, a new ligation state emerges with the spectroscopic characteristics of a pentacoordinated quantum mixed state of the heme iron. Gel electrophoresis revealed substantial formation of soluble dimers and trimers at submillimolar concentrations, whereas monomers were dominant at lower, micromolar concentrations. Ultraviolet circular dichroism spectra indicate that oxidized monomers are pre-molten globule to globule-like with a substantial fraction of secondary (helical) structure reminiscent of alkaline state V. The oligomers contain even more helical structure, which suggests domain swapping as the underlying mechanism of their formation. A substantial fraction of the submillimolar mixture of monomers and oligomers underwent a reduction of the heme iron. Its dependence on pH suggests the coupling to a proton transfer process. Altogether, our data indicate a partially unfolded ferricytochrome *c* conformation with spectroscopic characteristics reminiscent of the recently discovered alkaline isomer V_b, which is stabilized under folding conditions by exposing the protein to a very alkaline pH for an extended period of time.



For the past 20 years, cytochrome *c* has been utilized as an ideal model system for protein folding and unfolding studies.^{1–4} Results from various kinetic experiments suggest that the folding of denatured oxidized cytochrome *c* involves the population of an off-pathway kinetic intermediate state, in which the imidazole group of H33 rather than the functionally pivotal M80 is bound axially to the heme iron.⁴ The thus misfolded state is in equilibrium with an on-pathway state, in which the protein exhibits a hexacoordinated high-spin heme iron with water as the distal ligand. The latter eventually converts into the fully folded, “native”, conformation with Met80 as the proximal ligand (Figure 1) to complete the folding process. Recently, Tzul et al. revealed an even more complex picture for the folding pathway of ferric iso-1-cytochrome *c*, which depicts a competition between intramolecular histidine loop formation and ligand-mediated oligomer formation because of the binding of a histidine side chain of one molecule to the free binding site of another.⁵ Thus, the misligated kinetic intermediate can encompass monomers as well as soluble and partially folded oligomers. This finding is in line with earlier reported results from small-angle X-ray scattering, which suggest the formation of dimers during the refolding of horse heart cytochrome *c*.⁶ At equilibrium, i.e., folding (neutral pH and room temperature) or mildly unfolding conditions (high urea or guanidine hydrochloride concentration and room temperature), ferri- and ferrocytochrome *c* are both monomeric, but polymerization

by domain swapping can be thermodynamically achieved by dissolving the protein in ethanol/water mixtures.⁷

The occupation of a misfolded state is not an unusual part of the protein folding process. The energy landscape theory predicts that non-native interactions can trap proteins in kinetic intermediates along the unfolding pathway from which they can only slowly escape. However, as long as the Gibbs energy positions of such misfolded states remain above the glass transition point of the folding funnel, the barrier between the folded and misfolded state can be overcome on a subsecond time scale, thus allowing the fully folded state to become predominantly populated.⁸ For some proteins, the stability of the misfolded state can be increased by point mutations. The folding process of λ repressor fragment λ_{6-85} , for instance, shows a classical fast two-state kinetics, whereas its rather thermodynamically stable mutant (λ Q33Y) was found to exhibit an additional slow phase in which folding proceeds only on a millisecond time scale.^{9,10} The latter reflects a slowly decaying intermediate that was found to be rich in amyloid structure because of the presence of strong hydrophobic interacting intramolecular amyloids. Such kinetic traps have been found for the folding of many proteins, but frustrated

Received: November 26, 2012

Revised: January 31, 2013

Published: January 31, 2013



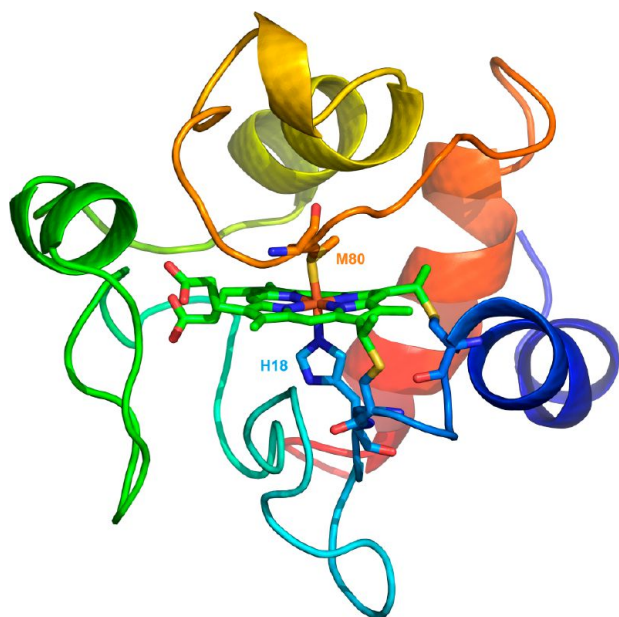


Figure 1. Structure of horse heart cytochrome *c* based on the coordinates from Protein Data Bank entry 1AAK in the oxidized form with axial ligands His18 and Met80 shown.⁷⁶

states from which a protein cannot escape on a measurable time scale are difficult to discover, because most proteins avoid them during the folding process. Some exceptions to this rule are serine protease inhibitors (serpins) and viral membrane fusion proteins, which remain in metastable states prior to reactions with other components of their respective environment.¹¹

In this paper, we report the discovery of what we consider to be a frustrated, misfolded state of cytochrome *c*, formed after the exposure of the oxidized protein to alkaline conditions for an extended period of time. We show that this state is very stable even under physiological conditions (pH 7 and room temperature). The majority of the proteins in our samples are predominantly monomeric at 0.05 mM but form substantial fractions of soluble dimers and higher-order oligomers at 0.5 mM, most likely because of domain swapping.^{5,7} Interestingly, fractions of this ensemble switch back into the reduced native state in a pH-dependent manner. Upon the addition of potassium ferricyanide to the sample, the protein is oxidized completely.

MATERIALS AND METHODS

Protein Preparation. Equine ferricytochrome *c*, from acetic acid, was obtained from Sigma-Aldrich and dissolved at a protein concentration of 0.5 or 0.05 mM in a 0.1 mM monobasic potassium phosphate buffer. We employed a sample preparation similar to a protocol previously developed by Alessi et al., which avoids photoreduction of the sample in resonance Raman experiments after its oxidation with $\sim 2 \mu\text{M}$ potassium ferricyanide $\{\text{K}[\text{Fe}(\text{CN})_6]\}$.¹² First, the pH of the sample was adjusted to 11.5 to neutralize the positive patches on the protein surface. Several lines of experimental evidence suggest that the protein adopts a partially unfolded state V under this condition.^{13–15} In a second step, the protein was allowed to stay at this pH for varying periods of time at 5 °C. A Sephadex G-25 (GE Healthcare) or G-75 (Pharmacia Fine Chemicals, Inc.) column was pretreated with a solution of potassium ferricyanide to compensate for the reducing nature of the

Sephadex gel. The protein solution was then passed over the column, which removes any excess oxidizing agent or other impurities.¹⁶ Finally, the pH of the eluted samples was titrated from 11.5 to various values between 11.5 and 4.0 using small aliquots of 0.1 M HCl or 0.1 M NaOH. The low molarity of the buffer ensured that the anion concentration was always below the region in which small anions can bind to the protein.^{17–19} The final concentration of cytochrome *c* was verified by measuring Soret band absorption.

Size Exclusion Gel Chromatography. The sample was passed over a Sephadex G-75 column (Pharmacia Fine Chemicals, Inc.) at room temperature. The column was pretreated with potassium ferricyanide to neutralize the reducing nature of the G-75 column. Aliquots were removed at regular intervals for electronic circular dichroism (ECD) and absorption measurements.

Protein Hydrolysis. Complete protein hydrolysis was achieved by producing a 3 M NaOH sample solution degassed with N_2 and heated for 8 h at 100 °C. After cooling, the alkali solution was neutralized with an equivalent amount of 1 M HCl prior to the adjustment of the sample to the pH of interest.²⁰

Gel Electrophoresis. Proteins were separated using a precast 4 to 20% polyacrylamide gel (Thermo Scientific) with Tris/glycine running buffer. Each well was loaded with 5 μL of the aqueous cytochrome *c* samples and run using a Mini-PROTEAN Tetra Cell (Bio-Rad) with a FB1000 power supply (Fisher), with a constant voltage (200 V and 20–50 mA) for ~ 30 min per gel. The protein molecular weight distribution was assessed with 5 μL of SeeBlue Plus2 Prestained Standard (Invitrogen). The gels were then stained using ProteoSilver Plus Silver stain (Sigma-Aldrich).

Absorption Spectroscopy. A Perkin-Elmer Lambda 35 UV–vis spectrometer was used to measure the spectra of the charge transfer (CT) region between 550 and 750 nm. We used a 10 mm quartz cell (Helma), with a data pitch of 0.1 nm, a continuous scanning speed of 480 nm/min, a response time of 1.0 s, and a bandwidth of 5 nm.

Circular Dichroism Spectroscopy. A Jasco J-810 spectropolarimeter continuously purged with N_2 was used to obtain visible and far-UV circular dichroism spectra (CD). Spectra of the Soret band region were recorded between 350 and 550 nm using a 1 mm quartz cell (Helma). The UV region was measured between 180 and 350 nm using a 0.05 mm Q silica demountable cell (International Crystal Laboratories). The spectra were all acquired using a data pitch of 0.1 nm, at a continuous scan speed of 200 nm/min, with a response time of 0.5 s and a bandwidth of 5 nm. A minimum of five accumulations for each pH were averaged at 20 °C.

Resonance Raman Spectroscopy. Polarized resonance Raman spectra were obtained using a Renishaw Ramascope (RM-1000), with a confocal Raman microscope (Olympus BH-2) equipped with a back-thinned CCD camera, a 2400 lines/mm grating, and a 50 \times microscope objective. Soret band resonance Raman spectra were collected using a HeCd laser (Kimmon) with an excitation wavelength of 441.6 nm. Aqueous cytochrome *c* samples were placed into a hanging drop microscope slide (Fisher) for acquisition. Spectra were collected with polarizations parallel (*x*) and perpendicular (*y*) to the polarization of the excitation laser beam. A minimum of five accumulations were collected for each spectrum at 20 °C and averaged.

RESULTS

A Non-Native Oxidized State Stabilized at Neutral pH.

Oxidized cytochrome *c* was prepared by using the protocol described in Materials and Methods. The oxidized protein was incubated at pH 11.5 and 4 °C for 2 h before we ran the sample over a Sephadex column pretreated with potassium ferricyanide. The protein concentration of the sample was 0.5 mM. Subsequently, we incrementally lowered the pH of the solution to various values between 8 and 5 and measured the corresponding optical absorption spectrum of the protein between 12500 and 18200 cm⁻¹. In this spectral region, one expects only a weak band at 14388 cm⁻¹, often termed the 695 nm band, which is now attributed to an S(M80) → d_π(Fe³⁺) rather than to an a_{2u}(heme) → d_π(Fe³⁺) charge transfer transition.^{21,22} This band, denoted as CT1 in the following, is indeed displayed in all spectra shown in Figure 2. Surprisingly,

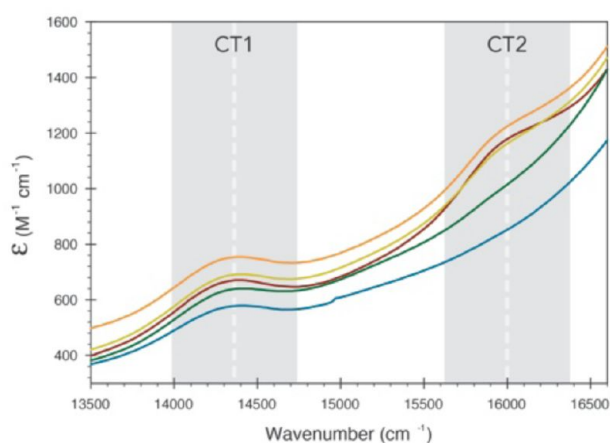


Figure 2. Charge transfer band region of the absorption spectrum of 0.5 mM ferricytochrome *c* (equine) measured between 13500 and 17000 cm⁻¹ at pH 5.0 (maroon), pH 5.5 (orange), pH 6.0 (olive), pH 7.0 (light green), and pH 8.0 (dark green) in 0.1 mM potassium phosphate buffer. Prior to the measurement, the oxidized protein was exposed to alkaline conditions (pH 11.5) for 2 h. Charge transfer bands CT1 and CT2 are explained in the text.

an additional weak band (CT2) appears at 16000 cm⁻¹ (625 nm) in the spectra measured below pH 6. Figure S1 of the Supporting Information shows the isolated CT1 and CT2 bands obtained from the spectra in Figure 2 after baseline subtraction. Apparently, the integrated intensity of CT1 is nearly pH independent, whereas the intensity of CT2 increases with a decrease in pH. We analyzed the CT2 band using our spectral decomposition program MULTIFIT²³ and found that it can be fit with a single Voigtian band. Figure 3 shows the integrated intensity of CT2 as a function of pH. The data clearly indicate a biphasic titration, which reflects the involvement of at least two amino acids with protonatable side chains. We fit the data using the titration model of Verbaro et al.,²⁴ which considered the influence of two different sets of interacting protonation sites on the oscillator strength of optical transitions. For pH-dependent oscillator strength f_{CT2} , this leads to the following equation:

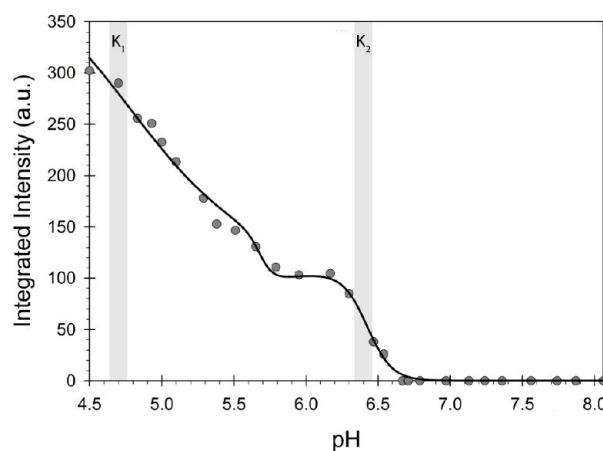


Figure 3. Integrated intensity of the CT2 band of horse heart ferricytochrome *c* incubated under oxidizing conditions at pH 11.5 for 2 h plotted as a function of pH. The solid curve results from a fit explained in the text.

$$f_{CT2}(pH) = f_{CT2}^{11} \left[1 + \left(\frac{K_1}{[H_3O^+]} \right)^{n_1} + \left(\frac{K_2}{[H_3O^+]} \right)^{n_2} + \frac{K_1^{n_1} K_2^{n_2}}{[H_3O^+]^{2(n_1+n_2)}} \right]^{-1} \\ + f_{CT2}^{10} \left[1 + \left(\frac{K_1}{[H_3O^+]} \right)^{n_1} + \left(\frac{[H_3O^+]}{K_2} \right)^{1/n_2} + \frac{K_1^{n_1}}{K_2^{n_2}} \right]^{-1} \\ + f_{CT2}^{01} \left[1 + \left(\frac{K_2}{[H_3O^+]} \right)^{n_2} + \left(\frac{[H_3O^+]}{K_1} \right)^{1/n_1} + \frac{K_2^{n_2}}{K_1^{n_1}} \right]^{-1}$$

This equation describes the two phases of the titration curve as cooperative processes, which involve the n_1 and n_2 protonations. The effective dissociation constants are K_1 and K_2 , respectively. f_{CT2}^{11} is the oscillator strength of the final fully protonated state, and f_{CT2}^{10} and f_{CT2}^{01} are the oscillator strengths of states in which one of the two considered groups is fully protonated. If $K_1 \gg K_2$, the third term of the equation contributes only weakly to f_{CT2} . To avoid any ambiguities, we assumed that $f_{CT2}^{10} = f_{CT2}^{01}$. The solid line in Figure 3 results from the fit to the data. The pK values related to K_1 and K_2 are 4.70 ± 0.07 and 6.40 ± 0.01 , respectively; for the Hill coefficients, we obtained the following values: $n_1 = 1$ (fixed parameter), and $n_2 = 3.9 \pm 0.6$. The value of the first coefficient indicates that only a single protonation step is involved; the second number reflects a high degree of cooperativity. It should be noted that the statistical error for pK₁ was underestimated because correlations between K_1 and f_{CT2}^{11} have not been taken into account.

The spectroscopic data described above suggest that our treatment of the protein caused the (weak) population of another state of cytochrome, which coexists with native state III and changes upon the protonation of amino acid residues. The appearance of the CT2 band at acidic pH indicates that this state is at least partially unfolded. We designate it as M to indicate the misfolded character of the protein's state. We call the three protonation states considered in the above equation M_{11} , M_{10} , and M_{01} . The deprotonated state is labeled as M_{00} . The appearance of the CT2 band is generally diagnostic of a hexacoordinated high-spin (hchs) state.²⁵ However, as we will argue below, resonance Raman and optical absorption data suggest that an alternative assignment must be considered.

The simultaneous occurrence of CT1 and CT2 in spectra taken at acidic pH suggests a mixture of folded and partially unfolded proteins. The protonated M states are formed by the protonation of a yet undetected non-native state M_{00} , which coexists with native state III at neutral pH. We wondered whether the data presented thus far were just a snapshot of a slow transition into state M_{00} . In this case, we should be able to isolate this state by increasing the incubation time of the protein under alkaline conditions. Therefore, we incubated ferricytochrome *c* for 7 days at pH 11.5 prior to measuring its absorption spectrum between 12500 and 18200 cm^{-1} (550–800 nm) as a function of pH. The observed spectra in Figure 4

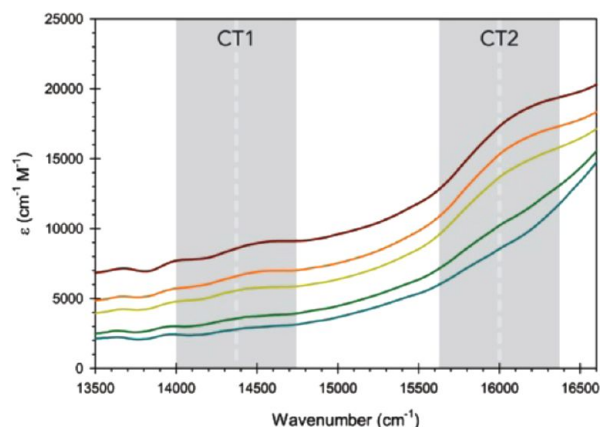


Figure 4. Charge transfer band region of the absorption spectrum of 0.5 mM ferricytochrome *c* (equine) measured between 13500 and 17000 cm^{-1} at pH 5.0 (maroon), pH 5.5 (orange), pH 6.0 (olive), pH 7.0 (light green), and pH 8.0 (dark green) in 0.1 mM potassium phosphate buffer. Prior to the measurement, the oxidized protein was exposed to alkaline conditions (pH 11.5) for 1 week. Charge transfer bands CT1 and CT2 are explained in the text.

do not depict the CT1 band, which clearly indicates the absence of native state III. The CT2 band appears again at acidic pH. Isolated bands obtained by background subtraction are shown in Figure S2 of the Supporting Information. We fit the equation given above to the pH dependence of the integrated intensity of CT2 depicted in Figure 5 and obtained

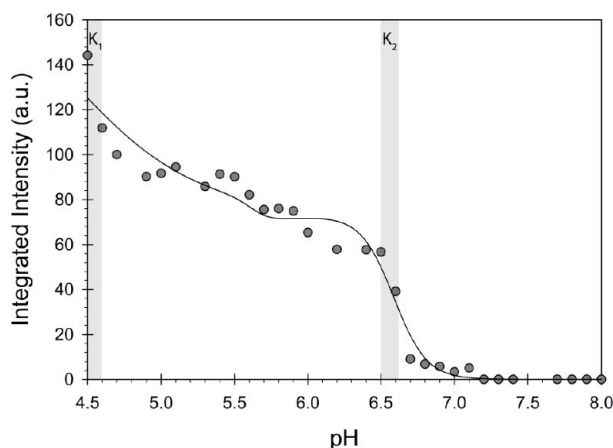


Figure 5. Integrated intensity of the CT2 band of horse heart ferricytochrome *c* incubated under oxidizing conditions at pH 11.5 for 7 days plotted as a function of pH. The solid curve results from a fit explained in the text.

the solid line depicted therein. The obtained pK values are 4.37 ± 0.25 and 6.58 ± 0.02 , and the Hill coefficients are as follows: $n_1 = 1$, and $n_2 = 3.9 \pm 0.7$. The oscillator strength f_{CT2}^{11} of 2150 $\text{M}^{-1} \text{cm}^{-2}$ is an order of magnitude larger than the corresponding value of 194 $\text{M}^{-1} \text{cm}^{-2}$ obtained from data in Figure 3, which indicates that only a small fraction (10%) of the proteins adopt state M after a 2 h incubation at alkaline pH.

Figure 6 shows the visible CD and absorption spectrum of the Soret band region, which were measured at pH 7 after

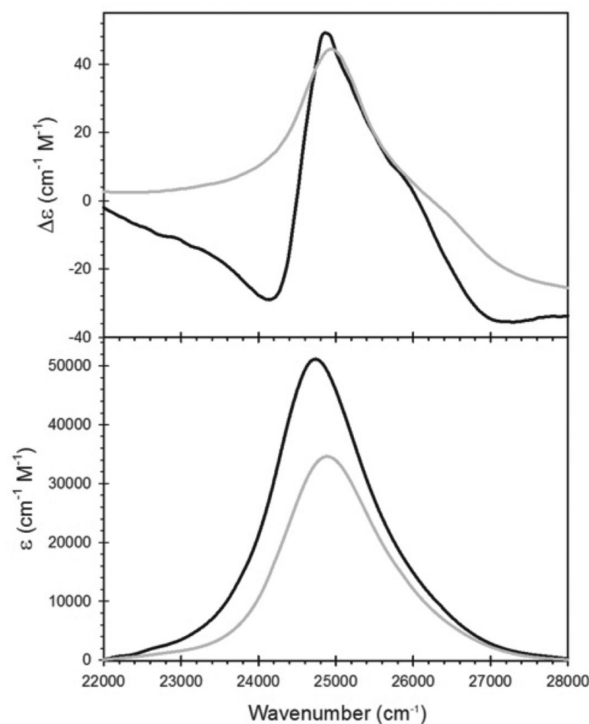


Figure 6. Circular dichroism (top) and absorption profile (bottom) of Soret band absorption of horse heart ferricytochrome *c* measured at the pH 7 after oxidation at pH 11.5 for 2 h (black) and 7 days (gray) under refrigerated conditions (5 °C).

exposure of the oxidized protein for 2 h and 7 days to alkaline conditions (pH 11.5), respectively. The visible CD spectrum taken after incubation for 2 h is still dominated by the classical couplet of the Soret band, which is indicative of an excited state splitting in protein state III.²⁶ The spectrum taken after oxidation for 1 week, however, shows a positive Cotton band that nearly coincides with the absorption band. This indicates the reduced splitting typical for partially unfolded states of the protein.²⁷ The corresponding absorption band is broadened and upshifted. Taken together, the spectroscopic data unambiguously show that the protein is now predominantly in the misfolded state of M.

Spectroscopic Characterization of State M. To further characterize the different protonation states of M, we measured the visible CD and absorption spectra of ferricytochrome *c* at several pH values between 11.5 and 5 after a 7 day incubation period at pH 11.5. The protein concentration for these measurements was 0.05 mM. Figure 7 shows positive Cotton bands for all CD spectra. This confirms that non-native states are populated at all these pH values. Interestingly, the intensities of the CD and the corresponding absorption bands are reminiscent of the respective band intensities that

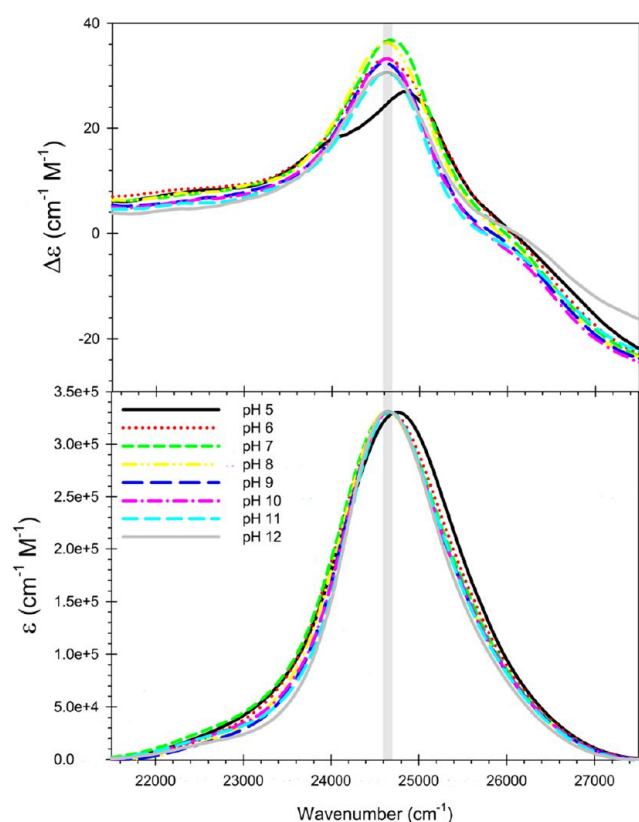


Figure 7. Circular dichroism (top) and absorption profile (bottom) of Soret band absorption of 0.05 mM horse heart ferricytochrome *c* measured at the indicated pH. Prior to the measurements, cytochrome *c* was subjected to conditions for 7 days at pH 11.5.

Hagarman et al. reported for state V of ferricytochrome *c*. This state exhibits much higher Soret band absorption and CD intensities than alkaline state IV or native state III.^{27,28} The CD profiles measured between pH 6 and 12 are all very similar, suggesting that the heme environment does not drastically change in this pH range. At pH 5, the CD band profile is clearly composed of two bands, which are red- and blue-shifted with respect to the position measured for the other pH values. The corresponding absorption spectrum is blue-shifted but does not coincide with the more intense sub-band of the CD profile. This could be indicative of the population of either a pentacoordinated high-spin ferric (pchs) state or, as we will argue below, a pentacoordinated quantum mixed (pcqm) state of the heme iron.²⁹ The thus detected conformational change at acidic pH is reminiscent of the $M_{00} \rightarrow M_{01/10} \rightarrow M_{11}$ transitions inferred from the appearance of the CT2 band in the 12500 and 18200 cm^{-1} region of the optical spectrum recorded with a 0.5 mM sample. It is difficult to infer this band from the spectrum of a sample with a concentration of 0.05 mM (Figure S3 of the Supporting Information), because this concentration is too low for probing weak charge transfer bands.

The noncoincidence between the absorption and CD profile indicates band splitting caused by electronic perturbations.³⁰ The low-wavenumber component of the CD spectrum does not have a discernible counterpart in the absorption spectrum. It is suspiciously close to the positive maximum observed in the CD spectrum of intact ferrocyanochrome *c*, which is slightly red-shifted from the peak position of the respective absorption band.²⁶ The other absorption spectra are all slightly blue-shifted from the peak position in the spectrum of native

ferricytochrome *c*. This is consistent with a hexacoordinated low-spin state.³¹

Ferricytochrome *c* in solution is known for its ability to adopt a variety of non-native conformations at nonphysiological pH or on the surface of anionic liposomes, in which the secondary structure is predominantly maintained.^{32–40} To probe the secondary structure of our M states, we measured the UV CD spectra at the same pH and for the same protein concentration used for the recording of the visible CD spectra. As shown in Figure 8, they clearly reveal a substantial fraction of secondary

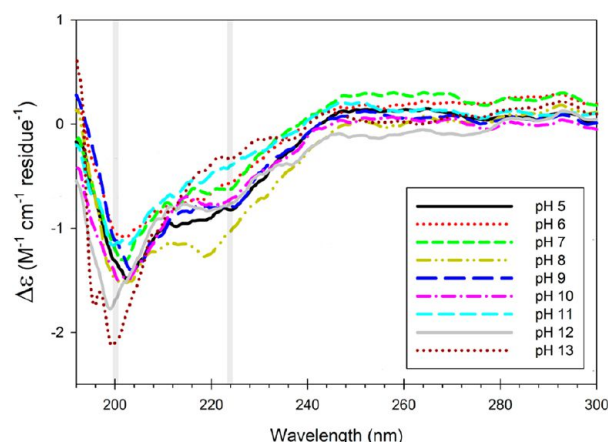


Figure 8. UV circular dichroism spectra 0.05 mM horse heart ferricytochrome *c* measured at the indicated pH. Prior to the measurements, cytochrome *c* was subjected to oxidizing conditions for 7 days at pH 11.5.

structure, which is predominantly α -helical. This view is confirmed by a more quantitative analysis performed with DichroWeb,^{41,42} using the CDSSTR⁴³ method with the SP175 reference set.⁴⁴ The result of this analysis is shown in Figure S4 of the Supporting Information. The obtained helical fraction of ~ 0.45 , which is practically pH-independent between pH 4 and 12 and decreases only at pH 13, is even slightly higher than the 40% helical fraction of the native state.⁴⁵ At pH 13, the protein unfolds into a statistical coil. The very weak negative maximum in the spectrum of the latter (1.9 mM cm^{-1} per residue) actually suggests a random coil state with a very reduced polypyrrolene II content.^{46,47}

Uversky recently showed that a so-called “double-wavelength plot” of $\Delta\epsilon_{222}$ versus $\Delta\epsilon_{200}$ can be utilized to further characterize the state of proteins (the author used molar ellipticities $[\theta]_{220}$ and $[\theta]_{200}$; we prefer the physically easier to interpret $\Delta\epsilon$ representation).⁴⁸ The author found that the data cluster in regions that can be identified as coil-like, pre-molten globule, molten globule, and globular. As shown in Figure 9, our data inferred from the spectra in Figure 8 all cluster in the transition region between the pre-molten globule and the globular region. This suggests a disordered state that lacks some of the native tertiary structure but still exhibits order on the secondary structure level.

We undertook an attempt to probe the resonance Raman spectrum of 0.05 mM state M ferricytochrome *c* at pH 5 and 7. Because our Raman microspectrometer does not allow the recording of spectra in the resonance region of the Soret band with a sufficiently good signal-to-noise ratio, we used the 442 nm excitation of our HeCd laser that provides preresonance excitation. We were able to identify the peak of the ν_4 band at 1371 cm^{-1} , which indicates an oxidized state (data not shown).

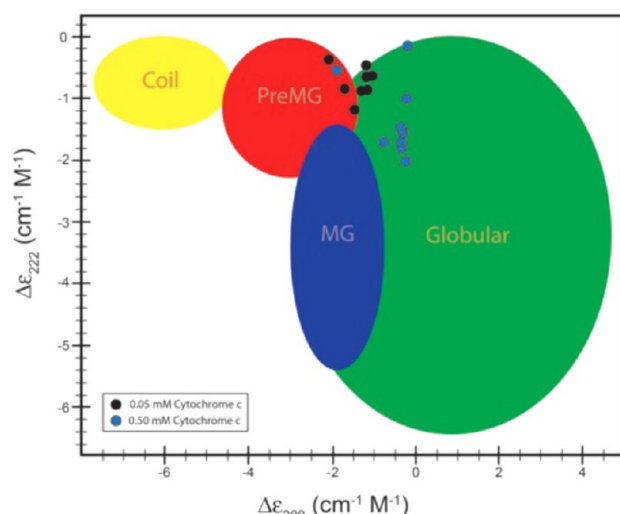


Figure 9. Analysis of UV circular dichroism spectra of 0.05 (black circles) and 0.5 mM (blue circles) horse heart ferricytochrome *c* taken at different pH values by means of a double-wavelength plot ($\Delta\epsilon_{222}$ vs $\Delta\epsilon_{200}$) as introduced by Uversky.⁴⁸ For all spectra analyzed, cytochrome *c* was subjected to oxidizing conditions at pH 11.5 for 7 days. The different colored areas of the plot indicate the location of pairs of $\Delta\epsilon_{222}$ and $\Delta\epsilon_{200}$ associated with statistical coil, pre-molten globule (PreMG), molten globule (MG), and globular structures.

Checking for Chemical Modifications. The data reported thus far clearly show that a very slow conformational transition occurs if one allows oxidized cytochrome *c* to remain at pH 11.5 for 1 week. To check for reversibility, we recorded another series of CD spectra after allowing the samples to stay for an additional 1 week at their respective pH values. The CD spectra depicted in Figure S5 of the Supporting Information show that no significant changes had occurred. One might therefore suspect that our findings reflect irreversible unfolding caused by chemical modifications of the protein rather than a conformational transition into a metastable state. It is known, for instance, that cytochrome *c*, if exposed to alkaline solutions, can form up to 15 deamidated species, which involves the conversion of asparagine and glutamine into asparaginy and glutaminy.⁴⁹ The most abundant deamidated species show a loss of the amides in the asparagine located at positions 52 and 54 of the protein. We checked our sample for deamidation by using a cation-exchange resin at neutral pH and found no indication of deamidation. Another possible chemical modification is hydrolyzation, which would produce protein fragmentation. If this had indeed occurred, one would expect a significant change in the secondary structure composition of our sample, because protein fragments would most likely be in a random or statistical coil state. To demonstrate this, we subjected cytochrome *c* to hydrolyzing conditions as described in Materials and Methods. When the protein was allowed to fully hydrolyze, the color of the sample converted from rust-colored to a green more viscous solution, which is clearly at variance with the spectra observed after oxidation for 1 week at alkaline pH. To check whether the recorded spectra could reflect partial hydrolysis, we probed the secondary structure of the sample subjected to hydrolyzing conditions as a function of time by measuring UV CD spectra of aliquots removed every 10 min (Figure S6 of the Supporting Information). We found that even the CD spectra taken after 10 min strongly suggest a statistical coil-like structure. This is in significant contrast to the

UV CD spectra of oxidized misfolded cytochrome *c* shown and discussed above (Figure 8).

To verify that our results are not caused by modifications of cytochrome *c* due to bacterial contamination of our sample, we added a drop of toluene at the start of the 1 week incubation period at pH 11.5. This did not lead to any significant changes in CD and absorption spectra.

Altogether, our tests show that the conformational transition induced at alkaline pH is not due to the discussed chemical modifications of the protein. Another possible chemical change, i.e., the oxidation of the M80 ligand, is discussed below.

Protein Aggregation. From what we have described thus far, the newly discovered M_{00} state still resembles partially unfolded alkaline state V.²⁷ As an unfolded or misfolded kinetic intermediate, this state is prone to aggregation into soluble dimers and higher-order oligomers.⁵ Therefore, the question of whether protein oligomers are formed under our experimental conditions arises. One might even go a step further by invoking the idea that irreversible aggregation is the prime reason for the population of state M. To check for protein aggregation of our 7 day incubation of the 0.05 mM sample, we conducted a native gel electrophoresis to determine the molecular weight distribution as a function of pH, shown in Figure 10. The

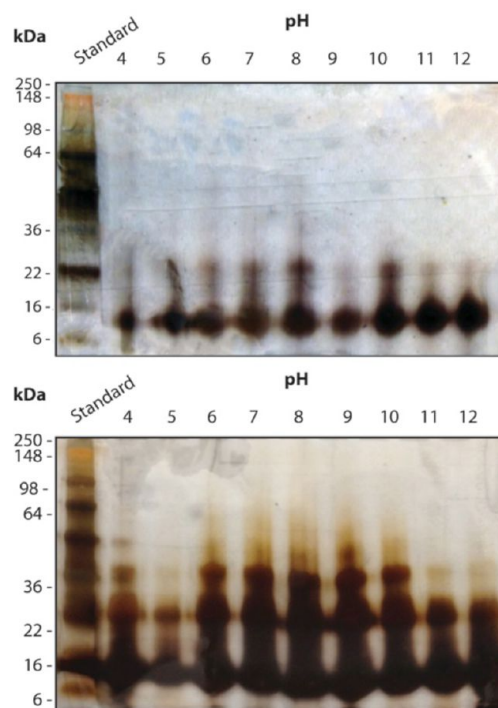


Figure 10. Images from gel electrophoresis of 0.05 (top) and 0.5 mM horse heart ferricytochrome *c* (bottom). The procedure was conducted after the protein had been subjected to oxidizing conditions at pH 11.5 for 7 days.

samples are dominated by protein monomers at all pH values investigated. A small fraction of dimers, however, indicates that soluble oligomers are indeed formed. This result clearly shows that oligomerization cannot be the cause of the irreversible formation of M and that its spectroscopic properties depicted in Figures 7 and 8 cannot be assigned to the monomeric protein. Furthermore, it reaffirms the notion that the protein has not undergone fragmentation due to hydrolysis.

Protein aggregation should be concentration-dependent. The low concentration of cytochrome *c* aggregates formed at 0.05 mM does not allow us to obtain the secondary structure of the formed dimers, so we repeated the set of experiments described above (absorption, visible and UV CD, and gel electrophoresis) with a 0.5 mM solution of ferricytochrome *c* after a 7 day incubation period at pH 11.5. The result of gel electrophoresis shown in Figure 10 reveals a mixture of monomers, dimers, and trimers. Oligomerization appears to be maximal in the pH range between 6 and 10, whereas the monomeric form remained dominant under acidic⁵ and alkaline conditions.^{11,12} The corresponding UV CD spectra are shown in Figure 11.

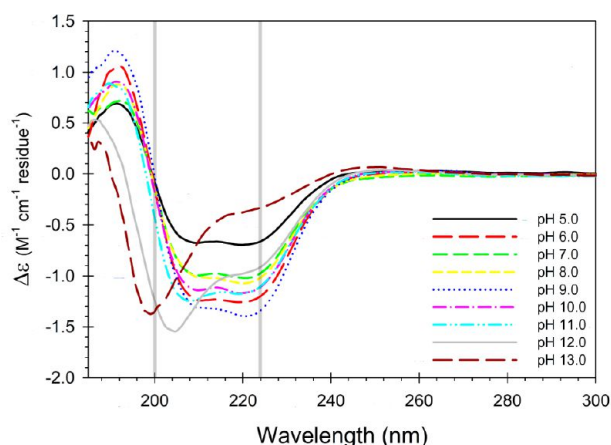


Figure 11. UV circular dichroism spectra of 0.5 mM horse heart ferricytochrome *c* measured at the indicated pH. Prior to the measurements, cytochrome *c* was subjected to oxidizing conditions for 7 days at pH 11.5.

They are very similar to the UV CD spectrum of the native protein,⁵⁰ which is clearly indicative of nearly intact secondary structures. This is confirmed by the result of our DichroWeb analysis displayed in Figure S7 of the Supporting Information. The $\Delta\epsilon_{222}$, $\Delta\epsilon_{200}$ coordinates in the Uversky plot in Figure 9 are now in the globular region, which corroborates the notion of very limited structural disorder in the oligomers. We can therefore conclude that the observed aggregation of cytochrome *c* does not involve the formation of β -sheet protofibrils. We propose that it is instead caused by domain swapping.^{7,51}

The visible CD and absorption spectra are rather complicated (data not shown). The reason is revealed by highly pH dependent visible Q-band spectra shown in Figure 12. The spectra taken at pH 7–10 all reflect a substantial amount of reduced ferrocytochrome *c*, suggesting that a fraction of proteins in our sample has switched back into the native state. We would like to remind the reader that our initial protocol had removed potassium ferricyanide by means of a Sephadex column after a short oxidation period at alkaline pH. The Q-band region of reduced cytochrome exhibits a clear separation of Q_0 and Q_π , with a higher peak intensity of the former,⁵² whereas Q_0 and Q_π merge into one single band in the spectra of all ferricytochrome *c* species, because of the reduced lifetime of the respective excited states.²² A comparison of the spectra in Figure 12 and the electrophoresis result displayed in Figure 10 suggests a correlation between oligomer formation and reduction. We therefore subjected a 0.5 mM sample of the protein to size exclusion chromatography as described in Materials and Methods. The Q-band spectra of different

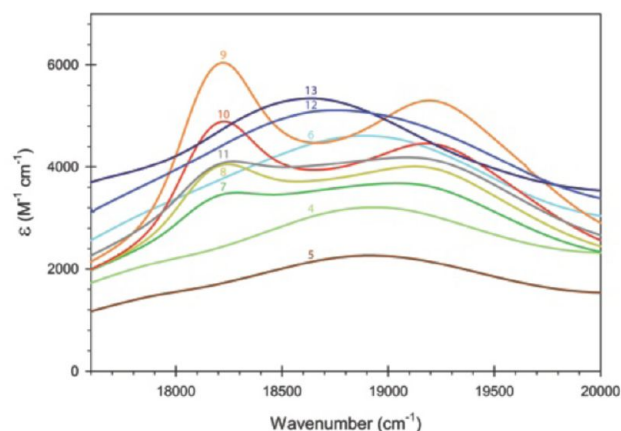


Figure 12. Q_0/Q_π band spectrum of 0.5 mM ferricytochrome *c* measured at the indicated pH after the protein had been subjected to oxidizing conditions at pH 11.5 for 7 days.

fractions are exhibited in Figure S8 of the Supporting Information. Apparently, the slower fractions (monomers and dimers) contain the highest fraction of reduced cytochrome *c*.

We measured the polarized resonance Raman spectrum of the 0.5 mM solution of ferricytochrome *c* after the 7 day incubation period at different pH values between 5 and 12. Overlaid spectra of x-polarized scattering are shown in Figure 13. Two bands are clearly displayed in the ν_4 , ν_3 , and ν_{10}

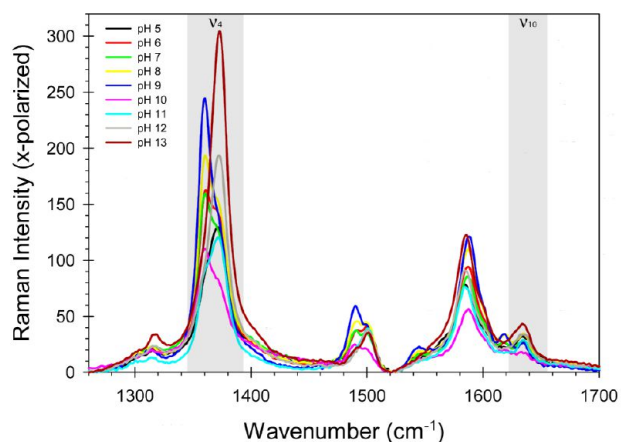


Figure 13. Resonance Raman spectra of 0.5 mM ferricytochrome *c* measured at the indicated pH after the protein had been subjected to oxidizing conditions at pH 11.5 for 7 days. The spectra were taken with 442 nm excitation.

regions of the spectrum, which are diagnostic of the coexistence of reduced and oxidized species.⁵³ We normalized the spectra onto the y component of ν_{21} at 1311 cm^{-1} and subsequently subjected all spectra to a self-consistent analysis by decomposing them into Lorentzian profiles with identical wavenumber positions and half-widths for the same bands in different spectra. All spectra can be described as a superposition of bands from oxidized and reduced hexacoordinated low-spin (hcls) species.^{14,53–55} The wavenumber positions of the classical marker modes of the oxidized species in Table 1 reveal a hcls state, in agreement with what we inferred from the absorption spectra of the 0.05 mM sample. Figure 14 shows relative intensities $I_{\text{red}}(\nu_4)$ and $I_{\text{ox}}(\nu_4)$ as a function of pH. The plotted data clearly indicate that the fraction of reduced cytochrome *c*

Table 1. Wavenumber Positions of Marker Bands in the Resonance Raman Spectrum of the Oxidized Fraction of Cytochrome *c* Incubated for 1 Week at pH 11.5 (column 2) and the Corresponding Bands in the Spectrum of State *V_b* Obtained by Döpner et al.¹⁴ (column 3)

mode	$\tilde{\nu}_M$ (cm ⁻¹)	$\tilde{\nu}_{V_b}$ (cm ⁻¹)
ν_4	1371	1370
ν_3	1499	1501
ν_2	1585	1586
ν_{10}	1635	1636

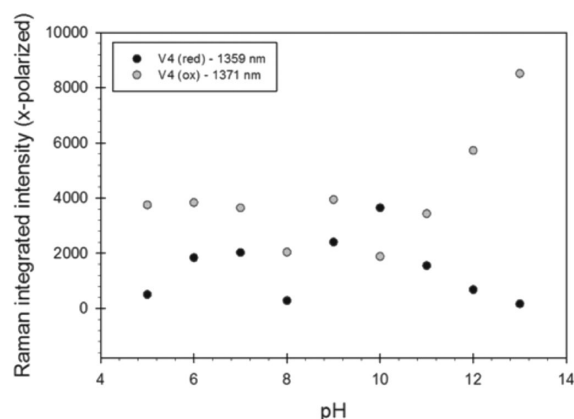


Figure 14. Integrated relative intensities of the ν_4 bands of oxidized and reduced proteins in the 0.5 mM sample of cytochrome *c* obtained after the proteins had been subjected to oxidizing conditions at pH 11.5 for 7 days. The data were obtained from a decomposition of the spectra exhibited in Figure 13.

becomes maximal at pH 9.00. Thus, the Raman data confirm the mixture of reduced and oxidized proteins that we inferred from the Q-band absorption spectra. Because the reduced state of cytochrome *c* requires M80 as an axial ligand, its occurrence rules out the possibility that state M is associated with the oxidation of the sulfur atom in M80. The possibility of such a modification of the M80 side chain is suggested by experiments that revealed the oxidation of the sulfur of free methionine into sulfoxide or an α -keto acid derivative under alkaline conditions.^{56,57}

DISCUSSION

It is well-known that ferricytochrome *c* is structurally a very flexible molecule. Seventy years ago, Theorell and Åkesson identified five distinct titration states populated between pH 1 and 12 that they designated with Roman numbers I–V.⁵⁸ State III is the so-called native, fully folded state. States IV and V are populated under alkaline conditions. Recent spectroscopic experiments by Verbaro et al. reported the population of an intermediate state III* at low ionic strengths.⁵⁹ The complete scheme therefore reads as



Subscripts a and b for states IV and V indicate the coexistence of different isomers.⁶⁰ In the study presented here, we exposed the protein to alkaline conditions at pH 11.5, at which state $V_{a,b}$ is predominantly populated. We found that cytochrome *c* under these conditions undergoes a very slow conformational transition from state V into state M, which refolded only after the formation of protein aggregates. A

spectroscopic comparison of the spectra of V and M (UV and visible CD) reveals only minor differences. This suggests that the respective secondary and tertiary structures are very similar. We can therefore propose the following scheme:



States M_{ij} (*i* and *j* = 0 or 1) have been introduced. States $M_{10/01}$ and M_{11} exhibit the CT2 band in their absorption spectra, though with different intensities. Because the measurements of the CT band spectra have been performed with a concentration of 0.5 mM, they might to a significant extent reflect the behavior of the protein oligomers, because a dominant fraction of the monomers seems to be in the reduced state.

The resonance Raman and absorption spectra of state M_{00} indicate a hcls state of the ferric heme iron for the predominantly monomeric 0.05 mM sample as well as for the oligomers formed at 0.5 mM. The classical candidates for the sixth ligand of a hcls complex are lysine (K72, K73, and K79)^{14,61} and histidine (H33 being the likely candidate).^{55,62} The position of the Soret band absorption (24900 cm⁻¹) is close to values generally observed for bis-histidine complexes of ferricytochrome *c*,^{31,63} whereas the respective lysine/histidine ligation leads to band positions at 24500 cm⁻¹.¹² However, as mentioned above, the respective CD spectra suggest that states V and M are very similar. As shown by Döpner et al., state V consists of two isomers termed V_a and V_b , which can be distinguished by means of the respective marker band frequencies in the resonance Raman spectrum. A comparison of the wavenumbers in Table 1 with the corresponding values of the V state isomers reported by Döpner et al. reveals that our data are close to those reported for isomer V_b , whereas the respective bands of V_a all appear at slightly higher wavenumbers than the bands in our M state Raman spectra. The same can be said about the marker bands in the Raman spectra of states IV (histidine/lysine complexes) and B (bis-histidine complexes).³¹ The spectral analysis of Döpner et al. revealed V_b to be much less populated than V_a . We therefore propose that the $V \rightarrow M$ transition is in fact a slow $V_a \rightarrow V_b$ transition.

The work of Döpner et al. has not led to a final identification of the sixth ligand in state V. However, several lines of reasoning led them to propose a hydroxyl ion as a ligand. Additional lines of evidence suggest that this is most likely the best candidate for our state $M = V_b$ in both its monomeric and oligomeric forms. First, the work of Hirota et al. provided spectroscopic evidence of OH⁻ being the sixth ligand in cytochrome *c* oligomers formed by domain swapping in an ethanol/water solution.¹⁴ Second, Silkstone et al. reported OH⁻ to be the sixth ligand in M80A and M80S ferricytochrome *c* mutants even at physiological pH.⁶⁴ We wonder whether the conformations produced by these mutations actually resemble misfolded state M or V_b .

The appearance of the CT2 band is normally indicative of a high-spin state of the metal iron,²⁵ but this notion is in conflict with the resonance Raman data, which still display the spin marker band close to their low-spin positions. However, all our experimental data can be sufficiently explained by invoking a pcqm state of the heme iron, which can be caused by spin–orbit coupling between a low-lying high-spin and a slightly higher intermediate spin state of the heme iron.^{65,66} The absorption spectrum of such a state would appear to be red-shifted with respect to that of all ferric hcls states but would have its peak still below 25000 cm⁻¹.²⁹ This is exactly what we

observed (Figure 7). The B-band peak position of a hexacoordinated high-spin state, however, lies at 25000 cm^{-1} (400 nm).⁶² The optical spectra of heme proteins with quantum mixed heme irons generally exhibit a charge transfer band in the CT2 region,²⁹ whereas the wavenumbers of the spin marker bands in the corresponding resonance Raman spectra are close to the respective low-spin values. Quantum mixed spin states have been found in cytochromes of the *c'* family and in class 3 peroxidases.^{65,67–69} A very prominent example is horseradish peroxidase.^{29,67,68,70} Quantum mixed states have not yet been discovered in cytochrome *c* derivatives (both native and unfolded), but one should keep in mind that cytochrome *c* on the surface of liposomes and on the inner membrane of mitochondria can acquire peroxidase activity, for which a quantum mixed state of the heme iron might be a prerequisite.^{29,69} The formation of the proposed pcqm state is triggered by the protonation of groups with pK values of 4.4 and 6.6. Our analysis of the CT2 titration suggests that the $M_{00} \rightarrow M_{01}$ transition exhibits a pK value of 6.5. This lies well in the region in which solvent accessible histidines are protonated. In cytochrome *c*, the sole candidate is H33.⁷¹ However, the high *n* values obtained from the fits suggest the involvement of three to four protons in the $M_{00} \rightarrow M_{10}$ transition. This indicates a network of interacting protonation sites. A possible candidate is one of the propionic acid peripheral substituents of the heme. In native cytochrome *c*, one of the respective pK values of the two propionic acids is unusually high (>9 for the other propionic acid),⁷² but it is more than likely that the respective pK value is lower in a partially unfolded state. We hypothesize that H33 and the outer propionate, which exhibits an alkaline pK value in folded cytochrome *c*, interact with the OH^- ligand to trigger the $M_{00} \rightarrow M_{01}$ transition. We propose that the second protonation step involves the protonation of the hydroxyl ligand. For the aforementioned M80A and M80S mutants of ferricytochrome *c*, the pK values of this reaction were reported to be 5.6 and 5.9, which are higher than the values of 4.3 and 4.7, respectively, inferred from our titration curves in Figures 3 and 5. However, our data in the region below pH 5 must be considered incomplete because we were not able to reach the saturation region below 4.0 because of the onset of aggregation-induced precipitation. It is possible that the data that can be assigned to the $M_{01/10} \rightarrow M_{11}$ transition involve, e.g., two protonation steps, with pK values below 4.0 and between 5.0 and 6.0. The first could be assigned to H26⁷² and the second to the protonation of OH^- .⁶⁵

The fact that the CT2 band is less intense in $M_{01/01}$ than in M_{11} suggests that it might in fact comprise a mixture of M_{00} and M_{11} rather than a thermodynamic intermediate between M_{00} and M_{11} . In other words, the protonations of H33, H26, and the outer propionic acid substituent change the equilibrium between two conformations with a hexacoordinated low-spin state and the pcqm state. The first protonation step produces a mixture of both states, whereas the second protonation stabilizes the pcqm state.

If our assessment of the ligation state of M or V_b is correct, one would expect that the protonation of the hydroxyl ligand should produce a hexacoordinated high-spin state with water as the sixth ligand. This is what the CT2 band alone would indicate. However, the pcqm state does fit into the picture as well, because a similar state in horseradish peroxidase exhibits a water molecule still close to the heme iron.⁷³

The observation of a pH-dependent fraction of reduced cytochrome *c* in the 0.5 mM sample is another really surprising

result. The pH dependence itself indicates coupling with protonation–deprotonation processes; i.e., the pK values of protonable groups are different in the oxidized and reduced state. As shown by Hauser et al., the heme carboxylate groups as well as lysine side chains are likely candidates.⁷⁴ The absence of reduced species in the monomer fraction of the 0.05 mM sample under neutral and alkaline conditions suggests that the electron transfer process must occur intermolecularly in oligomeric complexes. The heme reduction switches the protein to native state III. If this state is adopted in the oligomer, M80 might actually be provided by an adjacent cytochrome, as observed for cytochrome c_{552} . The newly formed state III monomers should establish a new equilibrium of reduced and oxidized proteins that reflect the corresponding redox potential.⁷⁵

Taken together, our data indicate that a metastable state of cytochrome *c* that can be described as an equilibrium between monomers and oligomers of pre-molten globule and globular proteins is stabilized at neutral pH. This suggests that the respective folding process has its transition region above the glass transition of the protein.⁸ If we allow the protein to undergo this very slow transition at pH 11, we change the folding landscape by lifting the glass transition above the transition region of the folding process along the pH coordinate. This is illustrated by the folding funnel in Figure 15. For yet unknown reasons, the thus formed ensemble of

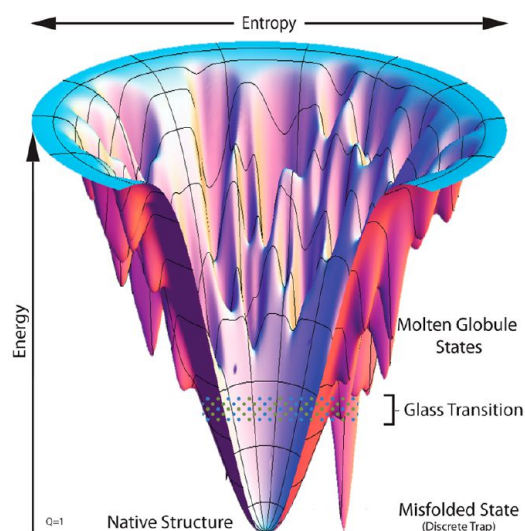


Figure 15. Feasible funnel-like protein folding landscape for a small helical protein. The preferred direction of flow is toward a unique native structure. When the glass transition temperature is higher than the folding temperature, the population of a frustrated misfolded state can occur over that of the native state.

protein monomers and oligomers establishes a dynamic equilibrium that involves the formation of reduced proteins in the pH range between 6 and 10.

■ ASSOCIATED CONTENT

Supporting Information

Additional figures of baseline-corrected absorption spectra, circular dichroism spectra, and calculated helical fractions. This material is available free of charge via the Internet at <http://pubs.acs.org>.

AUTHOR INFORMATION

Corresponding Author

*Phone: (215) 895-2268. Fax: (215) 895-1265. E-mail: rschweitzer-stenner@drexel.edu.

Funding

The project was supported in part by the Drexel College of Arts and Sciences and by a Maryanoff program summer stipend.

Notes

The authors declare no competing financial interest.

ACKNOWLEDGMENTS

We gratefully thank Dr. Carmichael Wallace for experimental assistance with the cation-exchange resin to test for deamidated species. We also thank Dr. Jun Xi for allowing access to his laboratory to perform the electrophoresis and Drs. Andrew Hagarman and Thomas Measey for training E.F. at the initial phase of the project.

ABBREVIATIONS

CT, charge transfer; CD, circular dichroism; PreMG, pre-molten globule state; hcls, hexacoordinated low-spin; hchs, hexacoordinated high-spin; pcqm, pentacoordinated quantum mixed.

REFERENCES

- (1) Elöve, G. A., Bhuyan, A. K., and Roder, H. (1994) Kinetic Mechanism of Cytochrome c Folding: Involvement of the Heme and Its Ligands. *Biochemistry* 33, 6925–6935.
- (2) Englander, S. W., Sosnick, T. R., Mayne, L. C., Shtilerman, M., Qi, P. X., and Bai, Y. W. (1998) Fast and slow folding in cytochrome c. *Acc. Chem. Res.* 31, 737–744.
- (3) Krishna, M. M. G., Maity, H., Rumbley, J. N., Lin, Y., and Englander, S. W. (2006) Order of steps in the cytochrome c folding pathway: Evidence for a sequential stabilization mechanism. *J. Mol. Biol.* 359, 1410–1419.
- (4) Yeh, S.-R., Takahashi, S., Fan, B., and Rousseau, D. L. (1997) Ligand exchange during cytochrome c folding. *Nat. Struct. Biol.* 4, 51–56.
- (5) Tzul, F. O., Kurchan, E., Roder, H., and Bowler, B. E. (2009) Competition between Reversible Aggregation and Loop Formation in Denatured Iso-1-cytochrome c. *Biochemistry* 48, 481–491.
- (6) Segel, D. J., Eliezer, D., Uversky, V. N., Fink, A. L., Hodgson, K., and Doniach, S. (1999) Transient Dimer in the Refolding Kinetics of Cytochrome c Characterized by Small-Angle X-ray Scattering. *Biochemistry* 38, 15352–15359.
- (7) Hirota, S., Hattori, Y., Nagao, S., Taketa, M., Komori, H., Kamikubo, H., Wang, Z., Takahashi, I., Negi, S., Sugiura, Y., Yataoka, M., and Higuchi, Y. (2010) Cytochrome c polymerization by successive domain swapping at the C-terminal helix. *Proc. Natl. Acad. Sci. U.S.A.* 107, 12854–12859.
- (8) Onuchic, J. N., Luthey-Schulten, Z., and Wolynes, P. G. (1997) Theory of Protein Folding: The Energy Landscape Perspective. *Annu. Rev. Phys. Chem.* 48, 545–600.
- (9) Liu, F., Gao, Y. G., and Gruebele, M. (2010) A Survey of λ Repressor Fragments from Two-State to Downhill Folding. *J. Mol. Biol.* 397, 789–798.
- (10) Liu, F., and Gruebele, M. (2007) Tuning λ 6–85 Towards Downhill Folding at its Melting Temperature. *J. Mol. Biol.* 370, 574–584.
- (11) Im, H., Woo, M.-S., Hwang, K. Y., and Yu, M.-H. (2002) Interactions Causing the Kinetic Trap in Serpin Protein Folding. *J. Biol. Chem.* 277, 46347–46354.
- (12) Alessi, M., Hagarman, A. M., Soffer, J. B., and Schweitzer-Stenner, R. (2010) In-plane deformations of the heme group in native

and nonnative oxidized cytochrome c probed by resonance Raman dispersion spectroscopy. *J. Raman Spectrosc.* 42, 917–925.

(13) Theorell, H., and Åkesson, Å. (1941) Studies on cytochrome c. *J. Am. Chem. Soc.* 63, 1804–1827.

(14) Döpner, S., Hildebrandt, P., Rosell, F. I., and Mauk, A. G. (1998) Alkaline Conformational Transitions of Ferricytochrome c Studied by Resonance Raman Spectroscopy. *J. Am. Chem. Soc.* 120, 11246–11255.

(15) Hagarman, A., Dutch, L., and Schweitzer-Stenner, R. (2008) The Conformational Manifold of Ferricytochrome c Explored by Visible and Far-UV Electronic Circular Dichroism Spectroscopy. *Biochemistry* 47, 9667–9677.

(16) Linder, R., Records, R., Barth, G., Bunnenberg, E., Djerassi, C., Hedlung, B. E., Rosenberg, A., Benson, E. S., Seamans, L., and Moscovitz, A. (1978) Partial Reduction of Aquomethemoglobin on a Sephadex G-25 Column as Detected by Magnetic Circular Dichroism Spectroscopy and Revised Extinction Coefficients of Aquomethemoglobin. *Anal. Biochem.* 90, 474–480.

(17) Battistuzzi, G., Loschi, L., Borsari, M., and Sola, M. (1999) Effects of nonspecific ion-protein interactions on the redox chemistry of cytochrome c. *J. Biol. Inorg. Chem.* 4, 601–607.

(18) Banci, L., Bertini, I., Redding, T., and Turano, P. (1998) Monitoring the conformational flexibility of cytochrome c at low ionic strength by H-NMR spectroscopy. *Eur. J. Biochem.* 256, 271–278.

(19) Shah, R., and Schweitzer-Stenner, R. (2008) Structural changes of horse heart ferricytochrome c induced by changes of ionic strength and anion binding. *Biochemistry* 47, 5250–5257.

(20) Aitken, A., and Learmonth, M. P. (2002) Quantitation of Tryptophan in Proteins. In *The Protein Protocols Handbook* (Walker, J. M., Ed.) 2nd ed., pp 41–44, Humana Press, Totowa, NJ.

(21) McKnight, J., Cheesman, M. R., Thomson, A. J., Miles, J. S., and Munro, A. W. (1993) Identification of charge transfer transitions in the optical spectrum of low-spin ferric cytochrome-P450 *Bacillus megaterium*. *Eur. J. Biochem.* 213, 683–687.

(22) Eaton, W. A., and Hochstrasser, R. M. (1967) Electronic Spectrum of Single Crystals of Ferricytochrome c. *J. Chem. Phys.* 46, 2533–2539.

(23) Jentzen, W., Ma, J.-G., and Shelnutt, J. A. (1998) Conservation of the Conformation of the Porphyrin Macrocycle in Hemoproteins. *Biophys. J.* 74, 753–763.

(24) Verbaro, D., Hagarman, A., Soffer, J., and Schweitzer-Stenner, R. (2009) The pH Dependence of the 695 nm Charge Transfer Band Reveals the Population of an Intermediate State of the Alkaline Transition of Ferricytochrome c at Low Ion Concentrations. *Biochemistry* 48, 2990–2996.

(25) Eaton, W., and Hochstrasser, R. M. (1958) Single-crystal spectra of ferrimyoglobin complexes in polarized light. *J. Chem. Phys.* 49, 985–995.

(26) Schweitzer-Stenner, R. (2008) The Internal Electric Field in Cytochrome c Explored by Visible Electronic Circular Dichroism Spectroscopy. *J. Phys. Chem. B* 112, 10358–10366.

(27) Hagarman, A., Dutch, L., and Schweitzer-Stenner, R. (2008) The Conformational Manifold of Ferricytochrome c Explored by Visible and Far-UV Electronic Circular Dichroism Spectroscopy. *Biochemistry* 47, 9667–9677.

(28) Schweitzer-Stenner, R., Hagarman, A., Verbaro, D., and Soffer, J. (2009) Conformational Stability of Cytochrome c Probed by Optical Spectroscopy. *Methods Enzymol.* 466, 109–153.

(29) Huang, Q., Szigeti, V., Fidy, J., and Schweitzer-Stenner, R. (2003) Structural Disorder of Native Horseradish Peroxidase Probed by Resonance Raman and Low Temperature Optical Absorption Spectroscopy. *J. Phys. Chem. B* 107, 2822–2830.

(30) Schweitzer-Stenner, R., Gorden, J. P., and Hagarman, A. (2007) The asymmetric band profile of the Soret band of deoxymyoglobin is caused by electronic and vibronic perturbations of the heme group rather than by a doming deformation. *J. Chem. Phys.* 127, 135103–135109.

- (31) Oellerich, S., Wackerbarth, H., and Hildebrandt, P. (2002) Spectroscopic Characterization of Nonnative Conformational States of Cytochrome c. *J. Phys. Chem. B* 106, 6566–6580.
- (32) Barker, P. D., and Mauk, A. G. (1992) pH-Linked conformational regulation of a metalloprotein oxidation-reduction equilibrium: Electrochemical analysis of the alkaline form of cytochrome c. *J. Am. Chem. Soc.* 114, 3619–3624.
- (33) Döpner, S., Hildebrandt, P., Rosell, F. I., and Mauk, A. G. (1998) The alkaline conformational transitions of ferricytochrome c studied by resonance Raman spectroscopy. *J. Am. Chem. Soc.* 120, 11246–11255.
- (34) Döpner, S., Hildebrandt, P., Rosell, F. I., Mauk, A. G., von Walter, M., Soulimane, T., and Buse, G. (1999) The structural and functional role of lysine residues in the binding domain of cytochrome c for the redox process with cytochrome c oxidase. *Eur. J. Biochem.* 261, 379–391.
- (35) Rossel, F. I., Ferrer, J. C., and Mauk, A. G. (1998) Proton-linked protein conformational switching: Definition of the alkaline conformational transition of yeast iso-1-ferricytochrome c. *J. Am. Chem. Soc.* 120, 11234–11245.
- (36) Battistuzzi, G., Borsari, M., Loschi, L., Martinelli, A., and Sola, M. (1999) Thermodynamics of the Alkaline Transition of Cytochrome c. *Biochemistry* 38, 7900–7907.
- (37) Gorbenko, G. P., Molotkovsky, J. G., and Kinnunen, P. K. J. (2006) Cytochrome c Interaction with Cardiolipin/Phosphatidylcholine Model Membranes: Effect of Cardiolipin Protonation. *Biophys. J.* 90, 4093–4103.
- (38) Rytömaa, M., and Kinnunen, P. K. J. (1994) Evidence for two Distinct Acidic Phospholipid-binding Sites in Cytochrome c. *J. Biol. Chem.* 269, 1770–1774.
- (39) Rytömaa, M., Mustonen, P., and Kinnunen, P. K. J. (1992) Reversible, Nonionic and pH-dependent Association of Cytochrome c with Cardiolipin-Phosphatidylcholine Liposomes. *J. Biol. Chem.* 267, 22243–22248.
- (40) Kapralov, A. A., Kurnikov, I. V., Vlasova, I. I., Belikova, N. A., Tyurin, V. A., Basova, L. V., Zhao, Q., Tyurina, Y. Y., Jiang, J., Bayir, H., Vladimirov, Y. A., and Kagan, V. E. (2007) The Hierarchy of Structural Transitions Induced in Cytochrome c by Anionic Phospholipids Determines Its Peroxidase Activation and Selective Peroxidation during Apoptosis in Cells. *Biochemistry* 46, 14232–14244.
- (41) Loble, A., Whitmore, L., and Wallace, B. A. (2002) DICHROWEB: An interactive website for the analysis of protein secondary structure from circular dichroism spectra. *Bioinformatics* 18, 211–212.
- (42) Whitmore, L., and Wallace, B. A. (2004) DICHROWEB, an online server for protein secondary structure analyses from circular dichroism spectroscopic data. *Nucleic Acids Res.* 32, W668–W673.
- (43) Sreerama, N., and Woody, R. W. (2000) Estimation of protein secondary structure from CD spectra: Comparison of CONTIN, SELCON, and CDSSTR methods with an expanded reference set. *Anal. Biochem.* 287, 252–260.
- (44) Lees, J. G., Miles, A. J., Wien, F., and Wallace, B. A. (2006) A reference database for circular dichroism spectroscopy covering fold and secondary structure space. *Bioinformatics* 22, 1955–1962.
- (45) Louie, G. V., and Brayer, G. D. (1990) High-resolution Refinement of Yeast Iso-1-Cytochrome c and Comparisons with Other Eukaryotic Cytochromes c. *J. Mol. Biol.* 214, 527–555.
- (46) Shi, Z., Woody, R. W., and Kallenbach, N. R. (2002) Is polyproline II a major backbone conformation in unfolded proteins? *Adv. Protein Chem.* 62, 163–240.
- (47) Hagarman, A., Measey, T. J., Mathieu, D., Schwalbe, H., and Schweitzer-Stenner, R. (2010) Intrinsic Propensities of Amino Acid Residues in GxG Peptides Inferred from Amide I band profiles and NMR Scalar Coupling Constants. *J. Am. Chem. Soc.* 132, 540–551.
- (48) Uversky, V. N. (2002) Natively Unfolded Proteins: A point where biology waits for physics. *Science* 11, 739–756.
- (49) Robinson, A. B., McKerrow, J. H., and Cary, P. (1970) Controlled Deamidation of Peptides and Proteins: An Experimental Hazard and a Possible Biological Timer. *Proc. Natl. Acad. Sci. U.S.A.* 66, 753–757.
- (50) Schweitzer-Stenner, R., Hagarman, A. M., Verbaro, D., and Soffer, J. B. (2009) Chapter Six: Conformational Stability of Cytochrome c Probed by Optical Spectroscopy. *Methods Enzymol.* 466, 109–153.
- (51) Yamasaki, M., Li, W., Johnson, D. J., and Huntington, J. (2008) Crystal structure of a stable dimer reveals the molecular basis of serpin polymerization. *Nature* 455, 1255–1258.
- (52) Friedman, J. M., Rousseau, D. L., and Adar, F. (1977) Excited state lifetimes in cytochromes measured from Raman scattering data: Evidence for iron-porphyrin interactions. *Proc. Natl. Acad. Sci. U.S.A.* 74, 2607–2611.
- (53) Hu, S., Morris, I. K., Singh, J. P., Smith, K. M., and Spiro, T. G. (1993) Complete Assignment of Cytochrome c Resonance Raman Spectra via Enzymatic Reconstitution with Isotopically Labeled Hemes. *J. Am. Chem. Soc.* 115, 12446–12458.
- (54) Spiro, T. G. (1993) *The resonance Raman spectra of metalloporphyrins and heme proteins*, Addison-Wesley, London.
- (55) Oellerich, S., Wackerbarth, H., and Hildebrandt, P. (2002) Spectroscopic characterization of nonnative conformational states of cytochrome c. *J. Phys. Chem. B* 106, 6566–6580.
- (56) Sharanabasamma, K., and Tuwar, S. M. (2010) Kinetics and mechanism of oxidation of DL-methionine by hexacyanoferrate(III) in aqueous alkaline medium. *J. Sulfur Chem.* 31, 177–187.
- (57) Shukla, R., and Upadhyay, S. K. (2008) Tween-80 catalysis in the oxidation of methionine and proline by alkane hexacyanoferrate(III). *Colloids Surf., A* 331, 245–249.
- (58) Theorell, H., and Åkesson, Å. (1939) Absorption Spectrum of Further Purified Cytochrome c. *Science* 90, 67.
- (59) Verbaro, D., Hagarman, A., Soffer, J. B., and Schweitzer-Stenner, R. (2009) The pH Dependence of the 695 nm Charge Transfer Band Reveals the Population of an Intermediate State of the Alkaline Transition of Ferricytochrome c at Low Ion Concentrations. *Biochemistry* 48, 2990–2996.
- (60) Döpner, S., Hildebrandt, P., Rosell, F. I., and Mauk, A. G. (1998) Alkaline Conformational Transitions of Ferricytochrome c Studied by Resonance Raman Spectroscopy. *J. Am. Chem. Soc.* 120, 11246–11255.
- (61) Blouin, C., Guillemette, J. G., and Wallace, C. J. A. (2001) Resolving the individual components of a pH-induced conformational change. *Biophys. J.* 81, 2331–2338.
- (62) Colón, W., Wakem, L. P., Sherman, F., and Roder, H. (1997) Identification of the Predominant Non-Native Histidine Ligand in Unfolded Cytochrome c. *Biochemistry* 36, 12535–12541.
- (63) Oellerich, S., Lecomte, S., Paternostre, M., Heimburg, T., and Hildebrandt, P. (2004) Peripheral and Integral Binding of Cytochrome c to Phospholipids Vesicles. *J. Phys. Chem. B* 108, 3781–3787.
- (64) Silkstone, G. G., Cooper, C. E., Svistunenko, D., and Wilson, M. T. (2005) EPR and Optical Spectroscopic Studies of Met80X Mutants of Yeast Ferricytochrome c. Models for Intermediates in the Alkaline Transition. *J. Am. Chem. Soc.* 127, 92–99.
- (65) Maltempo, M. M. (1976) Visible absorption spectra of quantum mixed-spin ferric heme proteins. *Biochim. Biophys. Acta* 434, 513–518.
- (66) Maltempo, M. M., and Moss, T. H. (1976) The spin 3/2 state and quantum spin mixtures in haem proteins. *Q. Rev. Biophys.* 9, 181–215.
- (67) Feis, A., Howes, B. D., Indiani, C., and Smulevich, G. (1998) Resonance Raman and electronic absorption spectra of horseradish peroxidase isoenzyme A2: Evidence for a quantum mix species. *J. Raman Spectrosc.* 29, 933–938.
- (68) Howes, B. D., Feis, A., Indiani, C., Morzocchi, M., and Smulevich, G. (2000) *J. Biol. Inorg. Chem.* 276, 40704–40711.
- (69) Howes, B. D., Schiødt, C. B., Welinder, K. G., Marzocchi, M. P., Ma, J.-G., Zhang, J., Shelnutt, J. A., and Smulevich, G. (1999) The quantum mixed spin heme state of barley peroxidase: A paradigm for class III peroxidases. *Biophys. J.* 77, 478–492.
- (70) Huang, Q., Al-Azzam, W., Griebenow, K., and Schweitzer-Stenner, R. (2003) Heme Structural Perturbation of PEG-Modified

Horseradish Peroxidase C in Aromatic Organic Solvents Probed by Optical Absorption and Resonance Raman Dispersion Spectroscopy. *Biophys. J.* 84, 3288–3298.

(71) Balakrishnan, G., Hu, Y., and Spiro, T. G. (2012) H26 Protonation in Cytochrome c Triggers Microsecond β -Sheet Formation and Heme Exposure: Implications for Apoptosis. *J. Am. Chem. Soc.* 134, 19061–19069.

(72) Bandi, S., and Bowler, B. E. (2011) Probing the Dynamics of a His73–Heme Alkaline Transition in a Destabilized Variant of Yeast Iso-1-cytochrome c with Conformationally Gated Electron Transfer Methods. *Biochemistry* 50, 10027–10040.

(73) Gajhede, M., Schuller, D. J., Heriksen, A., Smith, A. T., and Poulos, T. L. (1997) Crystal structure determination of classical horseradish peroxidase at 2.15 Å resolution. *Nat. Struct. Biol.* 4, 1032–1038.

(74) Hauser, K., Mao, J., and Gunner, M. R. (2004) pH Dependence of Heme Electrochemistry in Cytochromes Investigated by Multi-conformation Continuum Electrostatic Calculations. *Biopolymers* 74, 51–54.

(75) Hayashi, Y., Nagao, S., Osuka, H., Komori, H., Higuchi, Y., and Hirota, S. (2012) Domain Swapping of the Heme and N-Terminal α -Helix in *Hydrogenobacter thermophilus* Cytochrome c_{552} Dimer. *Biochemistry* 51, 8608–8616.

(76) Banci, L., Bertini, I., Gray, H. B., Luchinat, C., Reddig, T., Rosato, A., and Turano, P. (1997) Solution Structure of Oxidized Horse Heart Cytochrome c. *Biochemistry* 36, 9867–9877.